

A rhodamine/BODIPY-based fluorescent probe for the differential detection of Hg(II) and Au(III)^{†‡}

Erman Karakuş,§ Muhammed Üçüncü§ and Mustafa Emrullahoğlu*

Cite this: *Chem. Commun.*, 2014, 50, 1119Received 4th November 2013,
Accepted 19th November 2013

DOI: 10.1039/c3cc48436j

www.rsc.org/chemcomm

We described the design and synthesis of a molecular sensor based on a rhodamine/BODIPY platform that displayed differential fluorescence responses towards Hg²⁺ and Au³⁺ and demonstrated its utility in intracellular ion imaging.

In recent years, the construction of fluorescent molecular sensors for the detection of metal ion species has received a great deal of attention.¹ To date a large number of molecular sensors have been designed and developed, the majority of which are single-ion responsive and present no great challenge to researchers. Compared to single-ion responsive molecular sensors, however, the construction of multi-ion responsive molecular sensors with multiple emission modes are extremely challenging.² Molecular sensors displaying differential responses towards multiple ions are indispensable for designing molecular logic gates and molecular keypad lock devices.^{3,4}

The challenge of multiple analyte recognition presents several detection strategies. Incorporating multiple binding motifs onto a single sensing molecule, or alternatively, combining different transducing units (chromophores/fluorophores), allows for rapid access to molecular sensors with multiple emission modes.²

We envisaged that incorporating both a chemosensor and a chemodosimeter onto a single molecule could provide a suitable sensing platform for the differential detection of metal species. On the basis of this hypothesis, we constructed a molecular sensor possessing two different fluorophore units chemically integrated with each other. Both fluorophore units were elegantly designed to be non-emissive (*i.e.*, “off”) in their initial states and are expected to turn on respectively in response to the metal species of interest. To the best of our knowledge, molecular sensors based on this novel approach have not been covered in the literature.

Department of Chemistry, Faculty of Science, İzmir Institute of Technology (IZTECH), İzmir, Urla 35430, Turkey. E-mail: mustafaemrullahoglu@iyte.edu.tr

[†] Dedicated to the memory of Prof. Dr Ayhan S. Demir (1950–2012).

[‡] Electronic supplementary information (ESI) available: Synthesis and characterization of all compounds, and all data for UV-Vis and fluorescence titrations. See DOI: 10.1039/c3cc48436j

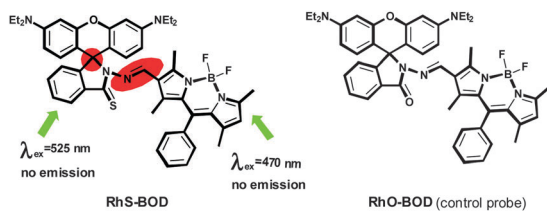
[§] These authors contributed equally to this work.

Ionic species of mercury (Hg²⁺) and gold (Au³⁺) share several similarities in terms of coordination properties. As both metal species show high affinities to thiols, they have the potential to interact with sulfur bearing biomolecules such as enzymes, proteins, and DNA. As a result, these metal species can disturb a series of cellular processes that lead to toxicity in humans.^{5,6} In recent years, a variety of well-designed fluorescent probes highly specific for Hg²⁺ and Au³⁺ ions have been developed, most of which are built on the exploitation of the thiophilic and alkynophilic behavior of these metal species.^{7,8} Despite impressive advances, many of these probes suffer from cross affinity. Because of their similar coordination properties, it is extremely difficult to construct a molecular sensor that differentiates between the Hg²⁺ and Au³⁺ species. To our knowledge, in the literature there is only one example of a fluorescent probe that can differentiate between Au³⁺ and Hg²⁺. This fluorescent probe, reported by Dong *et al.*, operates through a single emission mode and the differentiation is highly dependent on the sensing conditions.^{2d}

Obviously, there is a high demand for the development of molecular sensors that can differentiate multiple analytes of a similar chemical nature (*e.g.* Hg²⁺ and Au³⁺). In addition, small-molecule fluorescent sensors allowing the intracellular monitoring of multiple ions *via* differential responses are of high necessity for real-time cell imaging studies.

Herein, we present the design, synthesis, spectral properties, and cell imaging studies of **Rhs-BOD**, a new “turn-on” multi-fluorescent probe that allows the Hg²⁺ and Au³⁺ species to be differentiated on the basis of distinct fluorescence responses. **Rhs-BOD** constitutes a boron-dipyrromethene (BODIPY) dye and a spirocyclic rhodamine dye covalently attached to each other. **Rhs-BOD** was prepared in a reasonable yield (25%, overall) by the synthetic route outlined in Scheme S1 (see ESI[†]), and the structure of **Rhs-BOD** was confirmed by ¹H-NMR, ¹³C-NMR, and mass spectroscopy.

Importantly, the novel molecular sensor, **Rhs-BOD**, was designed in such a way that both of the fluorophore units are non-emissive before the addition of any metal species. As can be seen from the structure of the probe in Scheme 1, the C=N

Scheme 1 Structures of **RhS-BOD** and **RhO-BOD**.

functionality of the BODIPY core diminishes the BODIPY emission potentially because of a non-radiative deactivation process of the excited state through rapid isomerization of the C=N group. Similarly, the rhodamine fluorophore is non-emissive because the rhodamine dye exists in the ring closed isomeric form.

The sensing behavior of **RhS-BOD** towards the addition of different metal species was studied using UV-Vis and fluorescence spectroscopy. As shown in Fig. S1 (see ESI[†]), the UV-Vis spectrum of free **RhS-BOD** (CH₃CN/HEPES 1 : 1, pH 7.0) exhibits a single absorption band at 527 nm, which belongs to the BODIPY core. As the rhodamine core is in the ring closed isomeric form, we expect no absorption bands for the rhodamine derivative. However, the addition of Hg²⁺ (1 equiv.) to **RhS-BOD** led to the appearance of a new strong absorption band at 554 nm, which was assigned to a ring opened rhodamine derivative.

The fluorescence spectra of **RhS-BOD** displayed a similar behavior towards the addition of Hg²⁺ (Fig. 1). Initially, when excited at 525 nm there were no emission bands in the fluorescence spectrum of **RhS-BOD**. However, upon the addition of Hg²⁺, a new emission band with a maximum at 585 nm appeared and the intensity of this band gradually increased with an increasing concentration of Hg²⁺ (Fig. 1). The increase in emission intensity showed a linear relationship towards the addition of Hg²⁺ in the range of 0–0.3 μM. The minimum amount of Hg²⁺ was evaluated to be 8.0 nM under these conditions (Fig. S10, ESI[†]). The response of the probe towards the addition of Hg²⁺ was immediate and the emission intensity became saturated when 1 equiv. of Hg²⁺ was added, creating an enhancement factor of over 50-fold.

As expected, in the presence of Hg²⁺, **RhS-BOD** displayed the optical features of the rhodamine chromophore. During the process of adding Hg²⁺, no other accompanying emission bands were noticed in the emission spectrum that might belong to the BODIPY dye, indicating that the BODIPY dye was still in a sleep (“off”) mode.

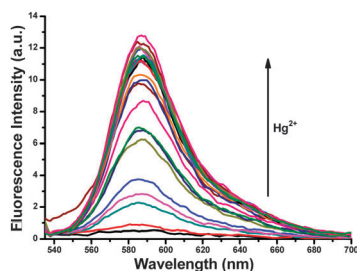


Fig. 1 Fluorescence spectra of **RhS-BOD** (5.0 μM) + Hg²⁺ (0.05 to 25.0 μM) in 1 : 1 CH₃CN/HEPES buffer (pH = 7.0) (λ_{ex} = 525 nm).

To check the reversibility of the Hg²⁺ sensing process, the highly emissive probe solution pre-treated with Hg²⁺ (**RhS-BOD**/Hg²⁺) was subsequently treated with a cyanide ion source (KCN or NH₄CN) (Fig. S7, ESI[†]). The probe solution immediately lost its color and its emission, thus showing that the sensing process is based on a reversible metal–ligand coordination process. The binding stoichiometry of the Hg²⁺/**RhS-BOD** association was determined by Job’s plot from both the UV-Vis absorption and fluorescence data (Fig. S9, ESI[†]). Both of the plots revealed that Hg²⁺ is associating with the probe in a 1 : 4 ratio.

We further investigated the selectivity profile of **RhS-BOD** in response to other metal ions. For all other metal cations, such as Cu²⁺, Ag⁺, Zn²⁺, Pb²⁺, Ni²⁺, Na⁺, Mg²⁺, Li⁺, K⁺, Pd²⁺, Fe²⁺, Co²⁺, Cd²⁺, Ca²⁺, Ba²⁺, Fe³⁺ and Cr³⁺, no detectable change in the emission intensity for **RhS-BOD** was observed (Fig. S5, ESI[†]). The probe was highly selective towards Hg²⁺ and showed no spectral response to any other metals ions, except for Au³⁺ ions. Upon the addition of Au³⁺, the non-emissive probe solution immediately turned to a strong green emissive solution that could be easily monitored by the naked eye under the UV lamp. A green emission was clear evidence of the existence of an emissive BODIPY derivative. This suggestion was also supported from the outcome of the reaction of **RhS-BOD** mediated by Au³⁺, as controlled using TLC. The formation of a green emissive compound, **BODIPY-AL**, could be easily monitored from the spots on the TLC plate (Fig. S21, ESI[†]).

The fluorescence sensing behavior of **RhS-BOD** towards Au³⁺ was comprehensively surveyed upon excitation at 470 nm and 525 nm. As shown in Fig. S11 (ESI[†]), the fluorescence spectrum of **RhS-BOD**/Au³⁺ (1 : 1) displays an emission band at 506 nm when excited at 470 nm, a characteristic emission band of a BODIPY fluorophore. On the other hand, the same probe solution (**RhS-BOD**/Au³⁺) when excited at 525 nm displays a different emission band at 585 nm, which is supposed to belong to the ring opened isomer of the rhodamine core (Fig. S13b, ESI[†]). The fluorescence emission intensity at both wavelengths increased linearly with an increasing concentration of Au³⁺ over a wide concentration range (Fig. 2 and Fig. S14, ESI[†]). The response of **RhS-BOD** towards Au³⁺ was fast (<1 min) and the emission intensity became saturated when 2 equiv. of Au³⁺ was added. In addition, the detection limit measured at both wavelengths was at the nM level (65 nM, λ_{em} = 585 nm and 10 nM, λ_{em} = 506 nm).

The fluorescence response of **RhS-BOD** toward Au³⁺ (1 equiv.) in the presence of other metal ions (10 equiv.) was explored in

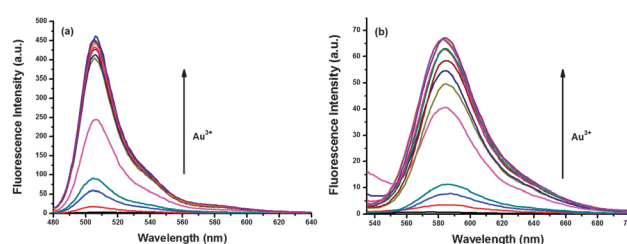
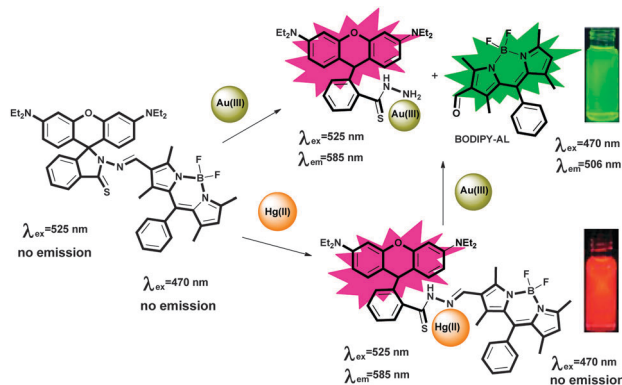


Fig. 2 Fluorescence titration spectra of **RhS-BOD** (5.0 μM) + Au³⁺ (0–10.0 equivalent) in 1 : 1 CH₃CN/HEPES buffer (pH = 7.0) (a) λ_{ex} = 470 nm, (b) λ_{ex} = 525 nm.



Scheme 2 Response of **RhS-BOD** towards the addition of Au^{3+} and Hg^{2+} .

order to assess the possible interference by other metal ions. As shown in Fig. S16 (see ESI†), the tested metal ions displayed no interference with the detection of Au^{3+} ions.

As discussed earlier, the addition of Hg^{2+} to **RhS-BOD** triggers a spiro-ring opening reaction and results in the formation of a highly emissive rhodamine derivative. Throughout the addition of Hg^{2+} to **RhS-BOD**, the BODIPY core continues to be non-emissive because the $\text{C}=\text{N}$ moiety was still preserved. However, the addition of Au^{3+} to the probe solution pre-treated with Hg^{2+} (**RhS-BOD**/ Hg^{2+}) resulted in an immediate change in the emission color from orange to green. Evidently, in the presence of Hg^{2+} and Au^{3+} , **RhS-BOD** hydrolyzes to give a green emissive BODIPY derivative, **BODIPY-AL**, which dominates the emission color of the probe solution (Scheme 2).

RhO-BOD, the oxygen bearing derivative of **RhS-BOD**, was used as the control probe to clarify the nature of the sensing process. Under the same sensing conditions, **RhO-BOD** displayed no response towards any metal species, indicating the indispensable role of the sulfur functionality in the detection of both metal species.

We next assessed the ability of **RhS-BOD** to operate within living organisms. To our delight, **RhS-BOD** showed the same

sensing behavior in living cells. Human A549 lung adenocarcinoma cell lines were incubated with the probe (5 μM) for 40 min and then followed by the addition of metal species. With the aid of fluorescence microscopy, the differential turn-on response towards Au^{3+} and Hg^{2+} was clearly monitored in the cells (Fig. 3). The images taken before and after the addition of the metal species displayed a distinct fluorescence change consistent with the results observed in the solution.

In conclusion, we have presented the synthesis, spectral properties, and biological applications of **RhS-BOD**, a new type of fluorescent probe for the differential detection of Hg^{2+} and Au^{3+} . This novel probe features excellent selectivity for Hg^{2+} and Au^{3+} . Detection of Hg^{2+} and Au^{3+} is realized through two distinct fluorescence changes resulting from Hg^{2+} -ligand coordination or from the hydrolysis of the $\text{C}=\text{N}$ moiety catalyzed by Au^{3+} . **RhS-BOD** exhibits a dual emission mode for the detection of Au^{3+} ions and a single emission mode for the detection of Hg^{2+} ions.

We thank İzmir Institute of Technology (IZTECH) and TUBITAK for financial support.

Notes and references

- (a) M. E. Jun, B. Roy and K. H. Ahn, *Chem. Commun.*, 2011, **47**, 7583; (b) H. Zheng, X.-Q. Zhan, Q.-N. Bian and X.-J. Zhang, *Chem. Commun.*, 2013, **49**, 429; (c) X. Chen, T. Pradhan, F. Wang, J. S. Kim and J. Yoon, *Chem. Rev.*, 2012, **112**, 1910; (d) G. Ulrich, R. Ziessel and A. Harriman, *Angew. Chem., Int. Ed.*, 2008, **47**, 1184; (e) N. Boens, V. Leen and W. Dehaen, *Chem. Soc. Rev.*, 2012, **41**, 1130.
- (a) L. Xue, Q. Liu and H. Jiang, *Org. Lett.*, 2009, **11**, 3454; (b) H. Komatsu, T. Miki, D. Citterio, T. Kubota, Y. Shindo, Y. Kitamura, K. Oka and K. Suzuki, *J. Am. Chem. Soc.*, 2005, **127**, 10798; (c) M. Yuan, W. Zhou, X. Liu, M. Zhu, J. Li, X. Yin, H. Zheng, Z. Zuo, C. Ouyang, H. Liu, Y. Li and D. Zhu, *J. Org. Chem.*, 2008, **73**, 5008; (d) M. Dong, Y.-W. Wang and Y. Peng, *Org. Lett.*, 2010, **12**, 5310; (e) D. Maity and T. Govindaraju, *Chem. Commun.*, 2012, **48**, 1039; (f) P. N. Basa and A. G. Sykes, *J. Org. Chem.*, 2012, **77**, 8428.
- (a) M. Kumar, R. Kumar and V. Bhalla, *Chem. Commun.*, 2009, 7384; (b) M. Suresh, A. Ghosh and A. Das, *Chem. Commun.*, 2008, 3906; (c) A. Misra, P. Srivastava and M. Shahid, *Analyst*, 2012, **137**, 3470.
- (a) U. Pischel, *Angew. Chem., Int. Ed.*, 2007, **46**, 4026; (b) A. P. De Silva and N. D. McClenaghan, *Chem.-Eur. J.*, 2004, **10**, 574; (c) K. Szacilowski, *Chem. Rev.*, 2008, **108**, 3481; (d) A. P. De Silva and N. D. McClenaghan, *J. Am. Chem. Soc.*, 2000, **122**, 3965; (e) D. Margulies, G. Melman, C. E. Felder, R. Arrad-Yellin and A. Shanzler, *J. Am. Chem. Soc.*, 2004, **126**, 15400; (f) S. J. Langford and T. Yann, *J. Am. Chem. Soc.*, 2003, **125**, 11198; (g) A. Coskun, E. Deniz and E. U. Akkaya, *Org. Lett.*, 2005, **7**, 5187; (h) S. Özlem and E. U. Akkaya, *J. Am. Chem. Soc.*, 2009, **131**, 48.
- I. Onyiko, A. R. Norris and E. Bunce, *Chem. Rev.*, 2004, **104**, 5911.
- E. Nyarko, T. Hara, D. J. Grab, A. Habib, Y. Kim, O. Nikolskaia, T. Fukuma and M. Tabata, *Chem.-Biol. Interact.*, 2004, **148**, 19.
- M. J. Culzoni, A. Muñoz de la Peña, A. Machuca, H. C. Goicoechea and R. Babiano, *Anal. Methods*, 2013, **5**, 30.
- (a) L. Yuan, W. Lin, Y. Yang and J. Song, *Chem. Commun.*, 2011, **47**, 4703; (b) J.-B. Wang, Q.-Q. Wu, Y.-Z. Min, Y.-Z. Liu and Q.-H. Song, *Chem. Commun.*, 2012, **48**, 744; (c) J. H. Do, H. N. Kim, J. Yoon, J. S. Kim and H.-J. Kim, *Org. Lett.*, 2010, **12**, 932; (d) H. Seo, M. E. Jun, O. A. Egorova, K.-H. Lee, K.-T. Kim and K. H. Ahn, *Org. Lett.*, 2012, **14**, 5062; (e) M. Emrullohoğlu, E. Karakuş and M. Üçüncü, *Analyst*, 2013, **138**, 3638; (f) J. Wang, W. Lin, L. Yuan, J. Song and W. Gao, *Chem. Commun.*, 2011, **47**, 12506; (g) N. T. Patil, V. S. Shinde, M. S. Thakare, P. H. Kumar, P. R. Bangal, A. K. Barui and C. R. Patra, *Chem. Commun.*, 2012, **48**, 11229; (h) Y.-K. Yang, S. Lee and J. Tae, *Org. Lett.*, 2009, **11**, 5610; (i) M. J. Jou, X. Chen, K. M. K. Swamy, H. N. Kim, H.-J. Kim, S.-G. Lee and J. Yoon, *Chem. Commun.*, 2009, 7218; (j) X. Cao, W. Lin and Y. Ding, *Chem.-Eur. J.*, 2011, **17**, 9066; (k) O. A. Egorova, H. Seo, A. Chatterjee and K. H. Ahn, *Org. Lett.*, 2010, **12**, 401.

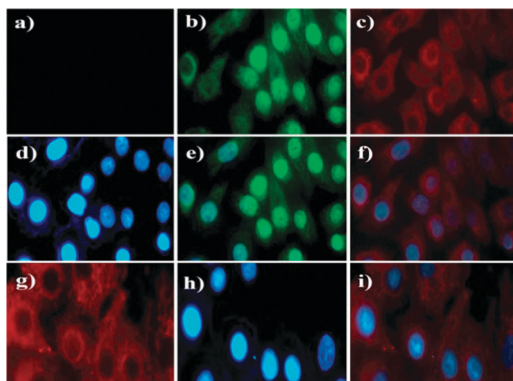


Fig. 3 (a) Fluorescence image of A549 cells treated with only **RhS-BOD** (5 μM); (b) image of cells treated with the probe (5 μM) and Au^{3+} (5 μM) ($\lambda_{\text{ex}} = 470 \text{ nm}$); (c) image of cells treated with the probe (5 μM) and Au^{3+} (5 μM) ($\lambda_{\text{ex}} = 525 \text{ nm}$); (d and h) images of cells treated with DAPI for 15 min (control); (d) merged image of frames (b) and (d); (f) merged image of frames (c) and (e); (g) image of cells treated with the probe (5 μM) and Hg^{2+} (5 μM) ($\lambda_{\text{ex}} = 525 \text{ nm}$); (i) merged image of frames (g) and (h).